Minimum-Fuel Powered Descent Guidance for Soft Landing on Irregular-Shaped Asteroids

Conference Paper · July 2015

DOI: 10.1109/ChiCC.2015.7260437

Yiyu Zheng
China Aerospace Science and Technology Corporation

Proceedings of the 34th Chinese Control Conference
July 28-30, 2015, Hangzhou, China

Minimum-Fuel Powered Descent Guidance for Soft Landing on Irregular-Shaped Asteroids

ZHENG Yiyu, CUI Hutao, TIAN Yang
Deep Space Exploration Research Center, Harbin Institute of Technology, Harbin 150001, P. R. China
E-mail: Banlamyu@gmail.com

Abstract: This work is concerned with the minimum-fuel power descent to a prescribed landing site on a irregular-shaped asteroid. With the small and complicated gravitational field taken into account, we present the equations of spacecraft motion in the asteroid-fixed Cartesian coordinate frame. To solve the minimum-fuel problem, we construct a performance index which links the minimum-fuel problem with the minimum-energy problem by a homotopy parameter. Based on the Pontryagin's maximum principle and the numerical continuation method, we transform the optimal control problem into a series of two-point boundary-value problems. we solve the optimal problems by starting from a solution of the energy-optimal problem, which is obtained by the using of the pseudo-spectral method. We reduce the homotopy parameter by following a certain series and take the solution obtained in the current iteration as an initial guess for that in the next one. Finally, we obtain a minimum-fuel power descent trajectory for soft landing on a irregular-shaped asteroid with easy convergence and high precision.

Key Words: Asteroid, soft landing, fuel-optimal trajectory, homotopy continuation

1 Introduction

The robotic space probe Rosetta was launched on 2 March 2004 and reached the comet 67P/Churyumov-Gerasimenko on 6 August 2014, becoming the first spacecraft to orbit a comet [1]. Rosetta's lander, Philae, touched down on the comet's surface on 12 November 2014. Philae is also the first spacecraft to land on a comet nucleus [2]. Because the gravity is so weak, there is a risk that the probe will rebound at the moment of touchdown. The lander has to rely on a system of harpoons to keep it locked to the surface [3]. The other two successful missions are the Near Earth Asteroid Rendezvous mission and Hayabusa sample return mission.

Due to the irregular shape of asteroids, accurate autonomous guidance is critical for safe and precise landing. To date, researchers have developed a number of guidance methods for soft landing on asteroids [4–12]. However, the fuel-optimal requirement is rarely taken into consideration. Using the Pontryagin's maximum principle (PMP), Guelman [13] presents a power-limit trajectory design method for asteroid landing. But the asteroid shape is assumed to be spherical. Taking the irregular shape of asteroid into account Lantoine [14] designs time-optimal and fuel-optimal trajectories for asteroid landing based on PMP (a indirect method for trajectory optimization). He also compares the calculation results solved by indirect method to that solved by the direct method. One can see from his paper that the indirect method has higher precision than the direct method in solving the optimal control problem of the asteroid landing.

The indirect method is a recommendable approach to obtain the fuel-optimal solution for the asteroid landing because the indirect method requires less computation cost and ensures hight solution precision. The PMP enables us to transform the optimal control problem into a two-point boundary-value problem (TPBVP). To approach the solution of the TPBVP, a initial guess needs to be given in advance [15]. However, the initial guess is very difficult to obtain due to following reasons: 1) the optimal solution for the fuel-optimal problem is of an Bang-Bang form; 2) The irregular shape of asteroids directly leads to a complicated gravitational field, which causes the dynamic equations of spacecraft in the body-fixed Cartesian coordinate frame have stronger nonlinearity; 3) To save the fuel, the spacecraft will shut off its engines during most of the power descent and keep free fall. Therefore, the soft landing is a long duration because the gravity is very weak. There are many different numerical methods such as the Newton-Raphson method, that can be employed to solve the TPBVP above. The solution of the fuel-optimal problem may not be obtained if a initial guess which is close to the solution can not be provided in advance. However, obtaining such a initial guess is quite difficult because the initial guess usually has no physical meaning.

This study presents a trajectory optimization method for the fuel-optimal soft landing on irregular-shaped asteroids, using a combination of the numerical continuation method [16–19], direct method and PMP. In the current document, the TPBVP that corresponds to the fuel-optimal soft landing on asteroids is expected to be easy to solve. To this end, we solve the fuel-optimal problem, of which the solution is difficult to obtain, by starting from a solution of the energy-optimal problem using the numerical continuation method. Note that the solution of the energy-optimal is relatively easy to obtain because the solution for such a problem is continues and is insensitive to the initial guess. Because the pseudo-spectral method is one of the typical representatives of the direct method and can solve a energy-optimal rapidly and accurately[20], the pseudo-spectral method is employed to solve the energy-optimal problem above. The solution for the energy-optimal problem enable us to start homotopy algorithm after we obtain it. To perform the homotopy algorithm, we reduce the homotopy parameter by following a certain series and take the solution obtained in the current iteration as an initial guess for that in the next one.

This work is sponsored by the Major State Basic Research Development Program of China (973 Program) through grant No. 2012CB720000 and National Natural Science Foundation of China (NSFC) through grant No. 61174201.

Corresponding author: ZHENG Yiyu, Ph.D. Candidate, Deep Space Exploration Research Center, E-mail: Banlamyu@gmail.com

Once the homotopy parameter is reduced to zero, we obtain a minimum-fuel power descent trajectory for the soft landing on a irregular-shaped asteroid. The trajectory optimization method presented in this paper takes full advantage of the characteristic of the energy-optimal solution's relative easy convergence and enable us the solve the fuel-optimal landing trajectory with high precision.

2 Guidance Problem Formulation

2.1 Dynamic Equation

As shown in Fig. 1, the asteroid-fixed Cartesian coordinate frame (x, y, z) and inertial Cartesian coordinate frame (X, Y, Z) share their origins at the center of mass, and have the same z-axis, about which it's assumed that the asteroid rotation speed is a constant rotation rate ω. The asteroid-fixed Cartesian coordinate frame aligns the x-, y-, and z-axes along the axes of minimum, intermediate, and maximum inertia respectively.

In the asteroid asteroid-fixed Cartesian coordinate frame,

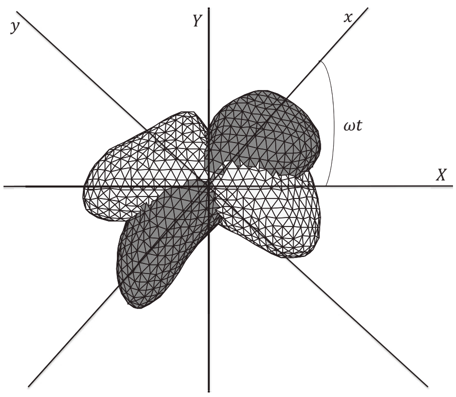

Fig. 1: Inertial and asteroid-fixed Cartesian coordinate frame relation [21].

the equations of the motion for the spacecraft can be written as follows [4, 5, 11]:

$$\ddot{x} = 2\omega\dot{y} + \omega^2 x + \frac{\partial U}{\partial x} + \frac{T_{\max}u}{m}\cos\beta\cos\theta \tag{1}$$

$$\ddot{y} = -2\omega\dot{x} + \omega^2 y + \frac{\partial U}{\partial y} + \frac{T_{\max}u}{m}\cos\beta\sin\theta \tag{2}$$

$$\ddot{z} = \frac{\partial U}{\partial z} + \frac{T_{\max}u}{m}\sin\beta \tag{3}$$

$$\dot{m} = -\frac{T_{\max}u}{I_{\mathrm{sp}}g_{\mathrm{e}}} \tag{4}$$

where $\boldsymbol{r} = [x, y, z]^{\mathrm{T}}$ and $\boldsymbol{v} = [\dot{x}, \dot{y}, \dot{z}]^{\mathrm{T}}$ are the position vector and velocity vector in the asteroid body-fixed Cartesian coordinate frame. $T_{\max}$ is the maximum thrust magnitude, $u \in [0, 1]$ is the thrust ratio. The angles β and θ serve as the thrust direction. I_{sp} is the thruster specific impulse, g_{e} is the Earth standard acceleration of gravity at sea level, 9.80665 $\mathrm{m/s^2}$. m is the instantaneous mass of the spacecraft. $\partial U/\partial x$, $\partial U/\partial y$ and $\partial U/\partial z$ are the components of the gradient of the gravitational potential U. The gravitational potential is modeled as a second-order spherical harmonic expansion given by [21]:

$$U = \frac{\mu}{r}\left\{1 + \left(\frac{r_a}{r}\right)^2\left[\frac{1}{2}C_{20}\left(\frac{3z^2}{r^2} - 1\right) + \right.\right. \\ \left.\left. +3C_{22}\frac{x^2 - y^2}{r^2}\right]\right\} \tag{5}$$

where μ is the product of constant of universal gravitation and the mass of target asteroid, r_a is the referenced radius, r is the distance from the mass center of target asteroid to the spacecraft.

The equations of the spacecraft motion can be written in a compact form:

$$\dot{\boldsymbol{r}} = \boldsymbol{v} \tag{6}$$

$$\dot{\boldsymbol{v}} = \boldsymbol{f}(\boldsymbol{r}, \boldsymbol{v}, \omega) + \partial U/\partial \boldsymbol{r} + T_{\max}u\boldsymbol{\alpha}/m \tag{7}$$

$$\dot{m} = -T_{\max}u/I_{\mathrm{sp}}g_{\mathrm{e}} \tag{8}$$

where

$$\boldsymbol{f}(\boldsymbol{r}, \boldsymbol{v}, \omega) = \begin{bmatrix} 2\omega\dot{y} + \omega^2 x \\ -2\omega\dot{x} + \omega^2 y \\ 0 \end{bmatrix}$$

and the unit vector of thrust direction

$$\boldsymbol{\alpha} = \begin{bmatrix} \cos\beta\cos\theta \\ \cos\beta\sin\theta \\ \sin\beta \end{bmatrix}$$

2.2 Boundary Conditions

The initial and final conditions are given by

$$\boldsymbol{r}(t_0) = \boldsymbol{r}_0, \boldsymbol{v}(t_0) = \boldsymbol{v}_0, m(t_0) = m_{\mathrm{wet}} \tag{9}$$

$$\boldsymbol{r}(t_f) = \boldsymbol{r}_f, \boldsymbol{v}(t_f) = \boldsymbol{v}_f, m(t_f) \geq m_{\mathrm{dry}} \tag{10}$$

where t_0 and t_f are the initial and final time, m_{wet} is the initial mass of the lander, m_{dry} is the mass of the lander without the propellant.

3 Minimum-Fuel Trajectory Design

The performance index J_{m} corresponds to the fuel-optimal problem is

$$J_{\mathrm{m}} = \frac{T_{\max}}{I_{\mathrm{sp}}g_{\mathrm{e}}}\int_{t_0}^{t_f} u\mathrm{d}t \tag{11}$$

and the performance index J_{e} corresponds to the energy-optimal problem is

$$J_{\mathrm{e}} = \frac{T_{\max}}{I_{\mathrm{sp}}g_{\mathrm{e}}}\int_{t_0}^{t_f} u^2\mathrm{d}t \tag{12}$$

To perform the homotopy algorithm, we construct a performance index as follow

$$J = \frac{T_{\max}}{I_{\mathrm{sp}}g_{\mathrm{e}}}\int_{t_0}^{t_f} (1 - \zeta)u + \zeta u^2 dt \tag{13}$$

where ζ is the homotopy parameter varying from 0 to 1.One can see that if $\zeta = 1$, then $J = J_{\mathrm{e}}$ and if $\zeta = 0$, then $J = J_{\mathrm{m}}$, which corresponds to the fuel-optimal problem. To obtain the solution for the fuel-optimal problem, one can solve a series of optimal control to minimize performance index J by varying parameter ζ from 1 to 0.

Based on the Pontryagin's maximum principle (PMP), we transform the optimal control problem into a two-point boundary-value problem (TPBVP).

The Hamiltonian of the system is built as

$$\begin{aligned} H =& \boldsymbol{\lambda}_r^{\mathrm{T}} \boldsymbol{v} + \boldsymbol{\lambda}_v^{\mathrm{T}} \left(\boldsymbol{f}(\boldsymbol{r}, \boldsymbol{v}, \omega) + \frac{\partial U}{\partial \boldsymbol{r}} + \frac{T_{\max} u}{m} \boldsymbol{\alpha} \right) \\ & - \lambda_m \frac{T_{\max} u}{I_{\mathrm{sp}} g_{\mathrm{e}}} + \frac{T_{\max}}{I_{\mathrm{sp}} g_{\mathrm{e}}} \left[(1-\zeta) u + \zeta u^2 \right] \end{aligned} \tag{14}$$

To minimize the Hamiltonian, the optimal thrust direction and magnitude should be determined by

$$\boldsymbol{\alpha}^* = -\boldsymbol{\lambda}_v / \|\boldsymbol{\lambda}_v\| \tag{15}$$

and

$$u^* = \begin{cases} u_0, & \zeta = 0 \\ u_\zeta, & \text{else} \end{cases} \tag{16}$$

where

$$u_\zeta = \begin{cases} 1, & S < -\zeta \\ 0.5 - 0.5S/\zeta, & |S| \le \zeta \\ 0, & S > \zeta \end{cases} \tag{17}$$

and

$$u_0 = \begin{cases} 1, & S < 0 \\ u_0 \in [0,1], & S = 0 \\ 0, & S > 0 \end{cases} \tag{18}$$

with the switching function

$$S = 1 - \lambda_m - \frac{I_{\mathrm{sp}} g_{\mathrm{e}} \|\lambda_v\|}{m} \tag{19}$$

The costate differential equations are

$$\dot{\boldsymbol{\lambda}}_r = -\frac{\partial H}{\partial \boldsymbol{r}} = -\left(\frac{\partial f(\boldsymbol{r}, \boldsymbol{v}, \omega)}{\partial \boldsymbol{r}} + \frac{\partial^2 U}{\partial \boldsymbol{r}^2} \right)^{\mathrm{T}} \boldsymbol{\lambda}_v \tag{20}$$

$$\dot{\boldsymbol{\lambda}}_v = -\frac{\partial H}{\partial \boldsymbol{v}} = -\boldsymbol{\lambda}_r - \left(\frac{\partial f(\boldsymbol{r}, \boldsymbol{v}, \omega)}{\partial \boldsymbol{v}} \right)^{\mathrm{T}} \boldsymbol{\lambda}_v \tag{21}$$

$$\dot{\lambda}_m = -\frac{\partial H}{\partial m} = -\frac{T_{\max} \|\lambda_v\|}{m^2} u \tag{22}$$

with the final condition

$$\lambda_m(t_f) = 0 \tag{23}$$

to be satisfied. Due to the free final time t_f, the transversality condition for Hamiltonian is

$$H(t_f) = 0 \tag{24}$$

Once the initial costates $[\boldsymbol{\lambda}_r(t_0), \boldsymbol{\lambda}_v(t_0), \lambda_m(t_0)]^{\mathrm{T}}$ and final time t_f are specified, one obtains the final value $\boldsymbol{r}(t_f)$, $\boldsymbol{v}(t_f)$, $\lambda_m(t_f)$ and $H(t_f)$ by integrating the equations of motion Eqs. (6)-(8) and the costate differential equations Eqs. (20)-(22) from $t = t_0$ to $t = t_f$. The final value should satisfy $\boldsymbol{r}(t_f) = \boldsymbol{r}_f, \boldsymbol{v}(t_f) = \boldsymbol{v}_f, \lambda_m(t_f) = 0$ and $H(t_f) = 0$. Therefore, we obtain a TPBVP:

$$\begin{cases} \dot{\boldsymbol{x}} = \boldsymbol{\phi}(t, \boldsymbol{x}, \zeta, u^*), t_0 \le t \le t_f \\ \boldsymbol{\rho}(\boldsymbol{x}(t_0), \boldsymbol{x}(t_f)) = 0, \end{cases} \tag{25}$$

where $\boldsymbol{x} = [\boldsymbol{r}, \boldsymbol{v}, m, \boldsymbol{\lambda}_r, \boldsymbol{\lambda}_v, \lambda_m]^{\mathrm{T}}$ and

$$\boldsymbol{\rho}(\boldsymbol{x}(t_0), \boldsymbol{x}(t_f)) = \begin{bmatrix} \boldsymbol{r}(t_f) - \boldsymbol{r}_f \\ \boldsymbol{v}(t_f) - \boldsymbol{v}_f \\ \lambda_m(t_f) \\ H(t_f) \end{bmatrix}$$

Considering that the TPBVP above can't be solved directly due to the unknown final time t_f, we define

$$\tau = t/t_f \tag{26}$$

then one has

$$\begin{cases} \frac{\mathrm{dx}}{\mathrm{d}\tau} = t_f \boldsymbol{\phi}(\tau, \boldsymbol{x}, \zeta, u^*), 0 \le \tau \le 1 \\ \boldsymbol{\rho}(\boldsymbol{x}(0), \boldsymbol{x}(1)) = 0, \end{cases} \tag{27}$$

where $\boldsymbol{x} = [\boldsymbol{r}, \boldsymbol{v}, m, \boldsymbol{\lambda}_r, \boldsymbol{\lambda}_v, \lambda_m]^{\mathrm{T}}$ and

$$\boldsymbol{\rho}(\boldsymbol{x}(0), \boldsymbol{x}(1)) = \begin{bmatrix} \boldsymbol{r}(1) - \boldsymbol{r}_f \\ \boldsymbol{v}(1) - \boldsymbol{v}_f \\ \lambda_m(1) \\ H(1) \end{bmatrix}$$

For a given parameter ζ, the shooting function is

$$\boldsymbol{F}(\boldsymbol{z}, \zeta) = [\boldsymbol{r}(1) - \boldsymbol{r}_f, \boldsymbol{v}(1) - \boldsymbol{v}_f, \lambda_m(1), H(1)]^{\mathrm{T}} = \boldsymbol{0} \tag{28}$$

where $\boldsymbol{z} = [\boldsymbol{\lambda}_r(\tau_0), \boldsymbol{\lambda}_v(\tau_0), \lambda_m(\tau_0), t_f]^{\mathrm{T}}$ is the combination of unknown initial costates and final time.

Varying parameter ζ from 1 to 0, we obtain a series of nonlinear equations $\boldsymbol{F}(\boldsymbol{z}, \zeta) = 0$. As mentioned above, the homotopy parameter ζ links the mass criterion ($\zeta = 0$) with the energy criterion ($\zeta = 1$). Let's assume that the initial solution $\boldsymbol{z} = \boldsymbol{z}^{(1)}$ for $\boldsymbol{F}\left(\boldsymbol{z}, \zeta^{(1)} = 1\right) = 0$ which corresponds to the energy-optimal problem has been obtained. Reducing the homotopy parameter ζ by following the certain series ($\zeta^{(1)}, \zeta^{(2)}, \zeta^{(3)}, ..., \zeta^{(*)} = 0$), and taking the solution obtained in the current iteration as an initial guess for that in the next one, the continuation method calculates further solutions

$$\left(\boldsymbol{z}^{(1)}, \zeta^{(1)}\right), \left(\boldsymbol{z}^{(2)}, \zeta^{(2)}\right), \left(\boldsymbol{z}^{(3)}, \zeta^{(3)}\right), ...,$$

until the target point ($\boldsymbol{z}^{(*)}, \zeta^{(*)}$) which corresponds to the fuel-optimal problem is reached. One can see that obtaining the solution $\boldsymbol{z}^{(*)}$ only requires the solution for the energy-optimal problem $\boldsymbol{z}^{(1)}$. Compared to the fuel-optimal problem, the energy-optimal problem is relative easy to solve. But it is also a challenge for us to find the solution because the initial costates are guessed within an unbounded space. Thus, to deal with this problem, we consider the adapting of the direct method.

Due to ease of implementation, the direct method has been widely adopted in engineering practice, especially in the field of trajectory optimization. The pseudo-spectral method is one of typical representatives of the direct method. It's recognized that the Karush-Kuhn-Tucker (KKT) conditions of Gauss pseudo-spectral method are equivalent with the one order optimality conditions of the maximum principle [20]. This enables us to obtain an initial costates guess for the energy-optimal problem $\boldsymbol{F}\left(\boldsymbol{z}, \zeta^{(1)} = 1\right) = 0$ using pseudo-spectral method to solve energy-optimal problem. Because the solution for energy-optimal problem is a continuous control, the rapid convergence and high precision of pseudo-spectral method can be achieved easily.

4 Numerical Results

To illustrate the effectiveness of the proposed minimum-fuel trajectory design method, in this section, a flight dynamics scenario simulating a spacecraft landing on 433 Eros is considered. The 3D model of 433 Eros is shown in Fig. 2. The model parameters of the asteroid in the landing phase are adopted from [5]. Other simulation conditions are specified by: $I_{\rm sp} = 300$ s, $T_{\max} = 20$ N, $m_{\rm wet} = 550$ kg, $\boldsymbol{r}_0 = [0.35, 0.30, 9.0]^{\rm T}$ km, $\boldsymbol{v}_0 = [-1.20, 0.20, -1.0]^{\rm T}$ m/s, $\boldsymbol{r}_f = [0, 0, 7.0]^{\rm T}$ km, $\boldsymbol{v}_f = [0, 0, 0]^{\rm T}$ m/s.

Fig. 2: 3D model of 433 Eros based on NEAR's Laser Rangefinder measurements [21].

Calculation results of the pseudo-spectral method for energy-optimal problem are shown in Fig. 3. It can be seen that both the thrust ration and thrust direction angles are continuous. The initial costates and final time $\boldsymbol{\lambda}_r(\tau_0)$, $\boldsymbol{\lambda}_v(\tau_0)$, $\lambda_m(\tau_0)$, and t_f for energy-optimal problem are shown in Tab. 1. They are used as an initial guess for the homotopy continuation method.

Calculation results of the homotopy continuation method

Table 1: Initial Costates and Final Time Guess Provided by Pseudo-Spectral Method

Initial Guess	Value
$\boldsymbol{\lambda}_r(\tau_0)$	$[-1.0457, 6.3518, 0.3939]^{\rm T}$
$\boldsymbol{\lambda}_v(\tau_0)$	$[-0.7578, 2.5356, -0.5177]^{\rm T}$
$\lambda_m(\tau_0)$	1.7407
t_f	1412.29 s

for the fuel-optimal problem are shown in Fig. 4–Fig. 8. Fig. 4 shows the position and velocity vectors $\boldsymbol{r}$ and $\boldsymbol{v}$ for the fuel-optimal problem. Fig. 5 shows the spacecraft mass m and Hamiltonian H. Finally, the propellant mass consumptions are nearly 1.4 kg. One can see that Hamiltonian is nearly zero throughout the trajectory. The very small deviation of the order of only 10^{-6} at certain intervals can be seen. The thrust ratio u and direction angle β and θ for the fuel-optimal problem is plotted in Fig. 6. Indeed, the optimal solution is a discontinuous Bang-Bang control. The spacecraft shuts off its engine during most of the power descent and keeps free fall. Fig. 7 shows the spacecraft trajectory during the power descent. Due to space limitations in this paper, only the initial value for λ_m changing with homotopy parameter ζ is plotted in Fig. 8. Initial value for λ_m changs continuously by the homotopy parameter. It indicates that the solution strategy of continuation method, taking the solution obtained in the current iteration as an initial guess for that in the next one, is reasonable.

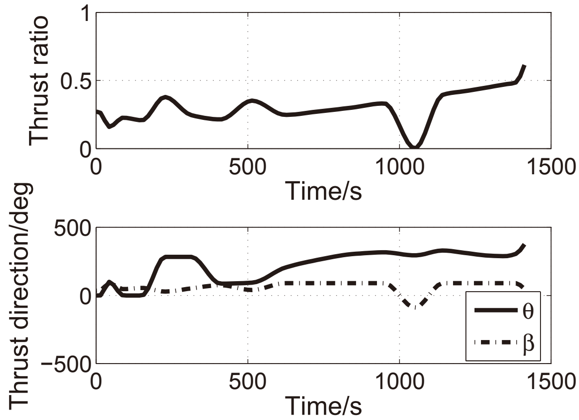

Fig. 3: Thrust ratio u and direction angle β and θ for the energy-optimal problem

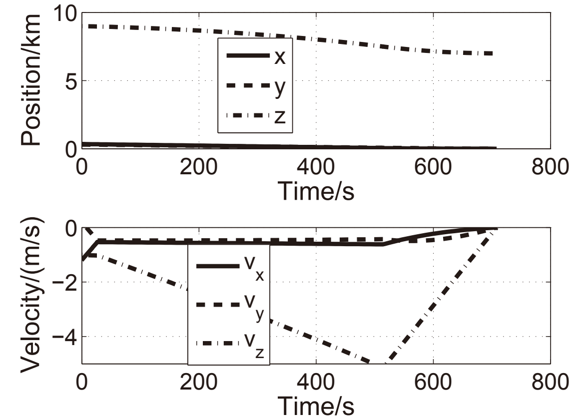

Fig. 4: Position and velocity vectors $\boldsymbol{r}$ and $\boldsymbol{v}$ for fuel-optimal problem.

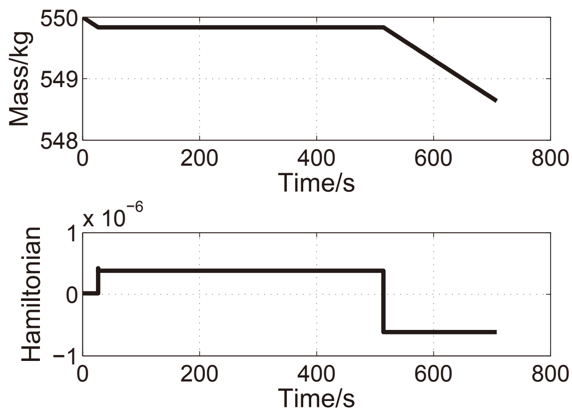

Fig. 5: Spacecraft mass m and Hamiltonian H for the fuel-optimal problem.

5 Conclusions

This paper presents a trajectory optimization method for the fuel-optimal soft landing on irregular-shaped asteroids,

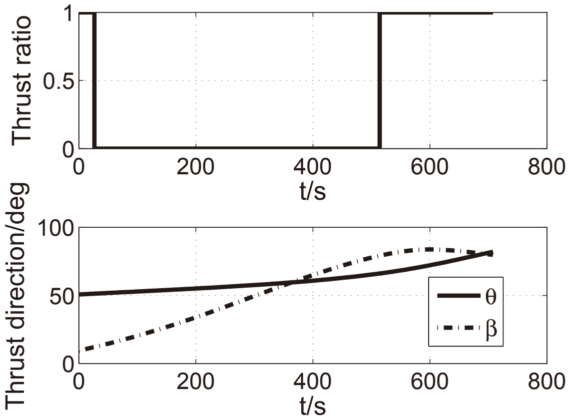

Fig. 6: Thrust ratio u and direction angle β and θ for the fuel-optimal problem.

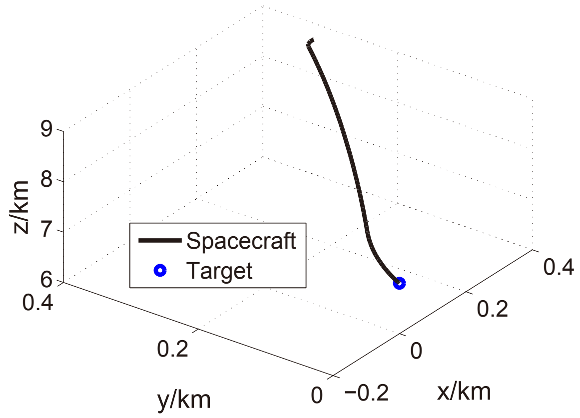

Fig. 7: Spacecraft trajectory for the fuel-optimal problem.

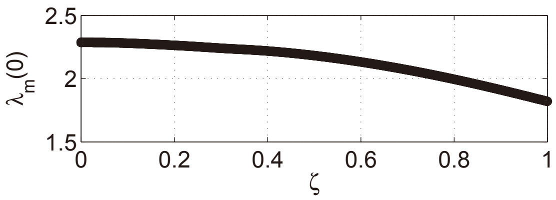

Fig. 8: Initial values for λ_m changing with the homotopy parameter ζ.

using a combination of the numerical continuation method, pseudo-spectral method and PMP. The numerical continuation method makes the TPBVP corresponds to the fuel-optimal soft landing on asteroids has a characteristic of easy convergence. We solve the fuel-optimal problem by starting from a solution of energy-optimal problem, of which solution is easy to obtain with the pseudo-spectral method. We find that the reduction of homotopy parameter should be small enough to ensure a stable convergence of numerical continuation. Simulation results show that the trajectory optimization method developed in this paper enables us to solve the minimum-fuel solution for the soft landing on irregular-shaped asteroids with easy convergence and high precision.

References

[1] K. H. Glassmeier, H. Boehnhardt, D. Koschny, et al. The Rosetta mission: flying towards the origin of the solar system. *Space Science Reviews*, 2007, 128(1-4): 1–21.

[2] E. Hand. Philae probe makes bumpy touchdown on a comet. *Science*, 2014, 346(6212): 900-901.

[3] Ulamec S, Biele J, Blazquez A, et al. Rosetta Lander-Philae: Landing preparations. *Acta Astronautica*, 2014, 107(2015):79–86.

[4] Kawaguchi J, Hashimoto T, Misu T, et al. An autonomous optical guidance and navigation around asteroids. *Acta astronautica*, 1999, 44(5): 267–280.

[5] Xiangyu H, Hutao C, Pingyuan C. An autonomous optical navigation and guidance for soft landing on asteroids. *Acta Astronautica*, 2004, 54(10): 763–771.

[6] Li S, Cui P Y. Landmark tracking based autonomous navigation schemes for landing spacecraft on asteroids. *Acta Astronautica*, 2008, 62(6): 391–403.

[7] Colin R M, Gianmarco R. Line-of-sight guidance for descent to a minor solar system body. *Journal of Guidance, Control, and Dynamics*, 1996, 19(3): 740–742.

[8] Li S, Cui P Y, Cui H T. Autonomous navigation and guidance for landing on asteroids. *Aerospace Science and Technology*, 2005, 10(3): 239–247.

[9] Lan Q, Li S, Yang J, et al. Finite-time soft landing on asteroids using nonsingular terminal sliding mode control. *Transactions of the Institute of Measurement and Control*, 2014, 36(2): 216–223.

[10] Yiyu Z, Hutao C, Xiaofang W. Robust dynamic surface control for soft landing on asteroids. *11th Academic Annual Meeting, Committee of Deep Space Exploration Technology, Chinese Society of Astronautics*, 2014.

[11] Furfaro R, Cersosimo D, Wibben D R. Asteroid precision landing via multiple sliding surfaces guidance techniques. *Journal of Guidance, Control, and Dynamics*, 2013, 36(4): 1075–1092.

[12] AI G, Pingyuan C, Hutao C. Robust guidance and control algorithms for small-body proximity operations based on constrained programming. *Systems Engineering and Electronics*, 2012, 34(5): 989–995.

[13] Guelman M, Harel D. Power limited soft landing on an asteroid. *Journal of guidance, control, and dynamics*, 1994, 17(1): 15-20.

[14] Lantoine G, Braun R, Lantoine G, et al. Optimal trajectories for soft landing on asteroids. 2006.

[15] Grant, M. J., Clark, I. G., Braun, R. D. Rapid entry corridor trajectory optimization for conceptual design. *AIAA Atmospheric Flight Mechanics Conference*, 2010.

[16] Bertrand R., Epenoy R. New smoothing techniques for solving bang-bang optimal control problems: numerical results and statistical interpretation. *Optimal Control Applications and Methods*, 2002, 23(4): 171–197.

[17] Wu T M. Solving the nonlinear equations by the Newton-homotopy continuation method with adjustable auxiliary homotopy function. *Applied mathematics and computation*, 2006, 173(1): 383–388.

[18] Wu T M. A study of convergence on the Newton-homotopy continuation method. *Applied Mathematics and Computation*, 2005, 168(2): 1169–1174.

[19] Guo T, Jiang F, Li J. Homotopic approach and pseudospectral method applied jointly to low thrust trajectory optimization. *Acta Astronautica*, 2012, 71: 38–50.

[20] D. Benson. A Gauss pseudo-spectral transcription for optimal control. *Massachusetts Institute of Technology*, 2005.

[21] Winkler T M. Fuel-efficient feedback control of orbital mo-

tion around irregular-shaped asteroids. *Iowa State University*, 2013.